

# Greedy routing on networks of mobile agents

Han-Xin Yang,<sup>1</sup> Wen-Xu Wang,<sup>2</sup> Ying-Cheng Lai,<sup>2</sup> and Bing-Hong Wang<sup>3</sup>

<sup>1</sup>*Department of Physics, Fuzhou University, Fuzhou 350002, China*

<sup>2</sup>*School of Electrical, Computer and Energy Engineering,  
Arizona State University, Tempe, AZ 85287, USA*

<sup>3</sup>*Department of Modern Physics, University of Science and Technology of China, Hefei 230026, China*

(Dated: November 11, 2018)

In this paper, we design a greedy routing on networks of mobile agents. In the greedy routing algorithm, every time step a packet in agent  $i$  is delivered to the agent  $j$  whose distance from the destination is shortest among searched neighbors of agent  $i$ . Based on the greedy routing, we study the traffic dynamics and traffic-driven epidemic spreading on networks of mobile agents. We find that the transportation capacity of networks and the epidemic threshold increase as the communication radius increases. For moderate moving speed, the transportation capacity of networks is the highest and the epidemic threshold maintains a large value. These results can help controlling the traffic congestion and epidemic spreading on mobile networks.

PACS numbers: 89.75.Hc, 05.70.Ln, 05.60.-k

## I. INTRODUCTION

Due to the increasing importance of communication networks such as the Internet [1] and networks of mobile phone users [2] in modern society, the traffic of information flows [3] and the spreading of computer viruses [4] in these networks have attracted more and more attention.

Traffic dynamics concern mainly how to effectively deliver information packets from source to destination on a network and avoid traffic congestion. The study of epidemic spreading focuses on the forecast and control of computer viruses. For a long time, the two types of dynamical processes were investigated separately. Recently, Meloni et al. [5] introduced a theoretical approach to incorporate traffic dynamics in virus spreading. In particular, they cast the susceptible-infected-susceptible (SIS) model [6] in a flow scenario where contagion is carried by information packets traveling across the network. A susceptible node is more likely to be infected if it receives more packets from infected neighbors. They found that the epidemic threshold depends on the traffic and decreases as traffic flow increases.

In communication networks, information packets are forwarded from sources to destinations by specific routing protocol. To enhance the the transportation capacity of communication networks, researchers have designed various routing algorithms, including the shortest path [7, 8], the integration of static and dynamic information [9], the local routing [10], the efficient routing [11], the greedy algorithm [12], and so on. It has been found that the routing algorithm also plays an important role in traffic-driven epidemic spreading [13, 14].

Previous studies about traffic dynamics usually focus on static networks, where nodes are motionless and links among nodes keep fixed. In our recent paper [15], we have studied the transportation dynamics on networks of mobile agents. We assume that agents move on a plane and the searching area of a agent  $i$  is a circle centered at  $i$ . In that paper, information packets were delivered according

to random routing algorithm, that is, a packet in agent  $i$  is forwarded to a randomly chosen agent  $j$  from agent  $i$ 's searching area. The random routing can be applied in the case where moving agents cannot obtain the information about other agents' positions. However, if an agent can know other agents' positions, the random routing is not an effective algorithm for a packet to quickly reach the destination. Utilizing the information of agents' positions, we now propose a greedy routing on networks of mobile agents. In the greedy routing, every time step a packet in agent  $i$  is delivered to the agent  $j$  whose distance from the destination is shortest among agent  $i$ 's searched neighbors. We have found that the greedy routing markedly enhances the transportation capacity of networks compared with random routing. Based on the greedy routing, we study how moving speed and communication radius affects traffic dynamics and traffic-driven epidemic spreading.

The paper is organized as follows. In Sec. II, we describe our model in terms of the greedy routing and epidemic spreading. Results on the traffic dynamics and the epidemic spreading are presented in Sec. III and Sec. IV respectively. A brief conclusion is given in Sec. V.

## II. MODEL

In our model,  $N$  agents move on a square-shaped cell of size  $L$  with periodic boundary conditions. Agents change their directions of motion  $\theta$  as time evolves, but the moving speed  $v$  is the same for all agents. Initially, agents are randomly distributed on the cell. After each time step, the position and moving direction of an arbitrary agent  $i$  are updated according to

$$x_i(t+1) = x_i(t) + v \cos \theta_i(t), \quad (1)$$

$$y_i(t+1) = y_i(t) + v \sin \theta_i(t), \quad (2)$$

$$\theta_i(t) = \Psi_i, \quad (3)$$

where  $x_i(t)$  and  $y_i(t)$  are the coordinates of the agent at time  $t$ , and  $\Psi_i$  is an  $N$ -independent random variable uniformly distributed in the interval  $[-\pi, \pi]$ .

Each agent has the same communication radius  $r$ . Two agents can communicate with each other if the distance between them is less than  $r$ . We define an agent  $i$ 's neighbors as agents who are within agent  $i$ 's communication area. At each time step, there are  $R$  packets generated in the system, with randomly chosen source and destination agents, and each agent can deliver at most  $C$  packet toward its destination. To transport a packet whose destination, an agent performs a local search within a circle of radius  $r$ . If the packet's destination is found within the searched area, it will be delivered directly to the destination. Otherwise, the packet is forwarded to a according to the greedy routing, which is defined as follows.

At time  $t$ , agent  $i$  has a packet whose destination is agent  $j$ . Agent  $k$  is one of  $i$ 's neighbors at that moment. The distance between agent  $k$  and agent  $j$  is

$$d_{jk}(t) = \sqrt{[x_j(t) - x_k(t)]^2 + [y_j(t) - y_k(t)]^2}. \quad (4)$$

Agent  $i$  will deliver the packet to the agent  $k$  whose distance  $d_{jk}(t)$  is shortest among agent  $i$ 's neighbors.

The queue length of each agent is assumed to be unlimited and the first-in-first-out principle holds for the queue. Once a packet reaches its destination, it will be removed from the system.

After a transient time, the total number of delivered packets at each time will reach to a steady value, then an initial fraction of agents  $\rho_0$  is set to be infected (e.g., we set  $\rho_0 = 0.1$  in numerical experiments). The infection spreads in the network through packet exchanges. For example, at time  $t$  agent  $i$  is infected and a packet is traveling from agent  $i$  to a susceptible agent  $j$ , then at the next time step, agent  $j$  will be infected with probability  $\beta$ . The infected agents are recovered at rate  $\mu$  (we set  $\mu = 1$  in this paper).

### III. TRAFFIC DYNAMICS

In this section, we study traffic dynamics based on the greedy routing. We set the number of agents  $N = 1500$ , the size of the square region  $L = 10$  and the delivering ability of each agent  $C = 1$  in this section.

To characterize the transportation capacity of a network, we exploit the order parameter  $\eta$  introduced in Ref. [16]:

$$\eta(R) = \lim_{t \rightarrow \infty} \frac{C \langle \Delta N_p \rangle}{R \Delta t}, \quad (5)$$

where  $\Delta N_p = N_p(t + \Delta t) - N_p(t)$ ,  $\langle \cdot \cdot \cdot \rangle$  indicates the average over a time window of width  $\Delta t$ , and  $N_p(t)$  represents the total number of information packets in the whole network at time  $t$ .

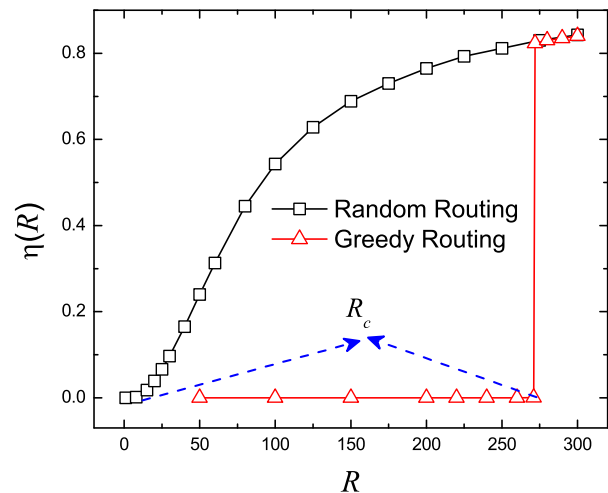


FIG. 1: (Color online) The order parameter  $\eta(R)$  as a function of the packet-generation rate  $R$  for random routing and greedy routing. For both routing algorithms, the moving speed  $v = 0.1$  and the communication radius  $r = 1$ .  $\eta(R)$  is obtained by averaging over  $5 \times 10^4$  time steps after disregarding  $5 \times 10^3$  initial steps as transients. Each data point results from an average over 50 different realizations.

As the packet-generation rate  $R$  is increased through a critical value of  $R_c$ , a transition occurs from free flow to congestion. For  $R \leq R_c$ , there is a balance between the number of generated and that of removed packets so that  $\langle \Delta N_p \rangle = 0$ , leading to  $\eta(R) = 0$ . In contrast, for  $R > R_c$ , congestion occurs and packets will accumulate in the system, resulting in a positive value of  $\eta(R)$ . The transportation capacity of a network can thus be characterized by the critical value  $R_c$ .

Figure 1 shows that the order parameter  $\eta(R)$  as a function of  $R$  for random routing and greedy routing. One can see that the critical value  $R_c$  for greedy routing is much larger than that of random routing when other parameters are the same. For the moving speed  $v = 0.1$  and the communication radius  $r = 1$ , the critical value  $R_c$  for random routing and greedy routing is about 8 and 270 respectively. This result shows that the greedy routing can greatly enhance the transportation capacity of networks in comparison with that of the random routing. In the following, we will detailedly study the traffic dynamics based on the greedy routing.

Figure 2 shows that the order parameter  $\eta(R)$  as a function of  $R$  for different values of  $v$  and  $r$ . One can see that both the moving speed and the communication radius affect the onset of traffic congestion. It is interesting to find that there are two different kinds of phase transition from free flow to congestion. When the moving speed is very small (i.e.,  $v = 0.001$ ), the jamming transition is a second-order phase transition. When the moving speed is large enough (i.e.,  $v = 0.1$  and  $v = 1$ ), the appearance of a congested phase belongs to a first-order phase transition.

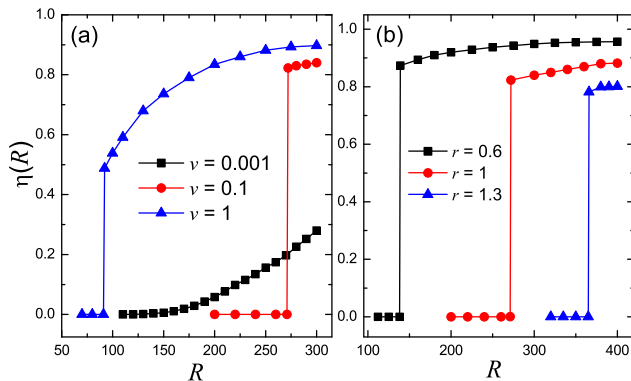


FIG. 2: (Color online) (a) The order parameter  $\eta(R)$  as a function of the packet-generation rate  $R$  for different values of the moving speed  $v$ . The communication radius  $r = 1$ . (b) The order parameter  $\eta(R)$  vs  $R$  for different values of  $r$ . The moving speed  $v = 0.1$ . Each data point results from an average over 50 different realizations.

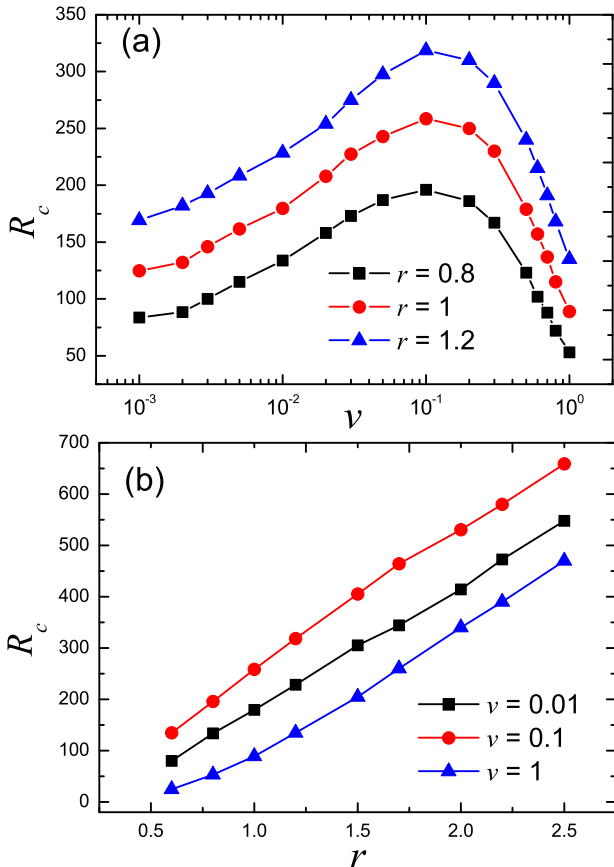


FIG. 3: (Color online) (a) The critical value  $R_c$  as a function of the moving speed  $v$  for different values of the communication radius  $r$ . (b) The dependence of  $R_c$  on  $r$  for different values of  $v$ . Each data point results from an average over 50 different realizations.

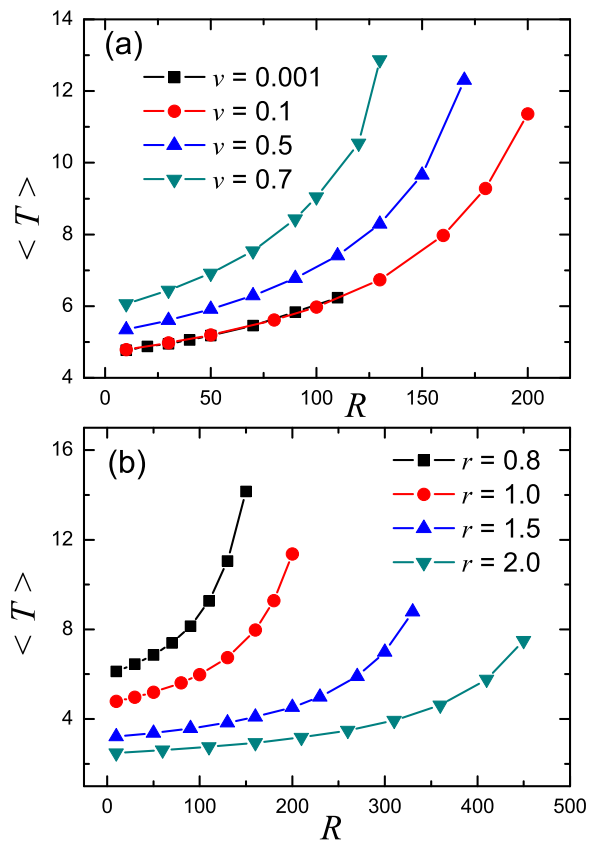


FIG. 4: (Color online) (a) The average traveling time  $\langle T \rangle$  as a function of the packet-generation rate  $R$  ( $< R_c$ ) for different values of the moving speed  $v$ . The communication radius  $r = 1$ . (b) The dependence of  $\langle T \rangle$  on  $R$  for different values of  $r$ . The moving speed  $v = 0.1$ .

Since the transportation capacity of networks is characterized by the critical value  $R_c$ , it is of particular interest for us to study how  $R_c$  is affected by the moving speed  $v$  and the communication radius  $r$ . Figure 3(a) shows the dependence of  $R_c$  on  $v$  for different values of  $r$ . One can observe a nonmonotonic behavior. For a fixed value of  $r$ , the largest value of  $R_c$  is obtained when the moving speed  $v$  is moderate (about 0.1). This result is different from that of Ref. [15], where  $R_c$  increases as  $v$  increases for random routing. Figure 3(b) shows the dependence of  $R_c$  on  $r$  for different values of  $v$ . One can see that,  $R_c$  increases as the communication radius  $r$  increases regardless of the values of  $v$ .

To understand how the moving speed and communication radius affect the transportation capacity of networks, we study the average traveling time  $\langle T \rangle$  and the load distribution  $P(n)$  in the next.

The average traveling time  $\langle T \rangle$  is defined as the average time steps for a packet traveling from source to destination. We investigate the average traveling time  $\langle T \rangle$  as a function of the packet-generation rate  $R$  in the free flow state ( $R \leq R_c$ ). From Fig. 4, one can find that

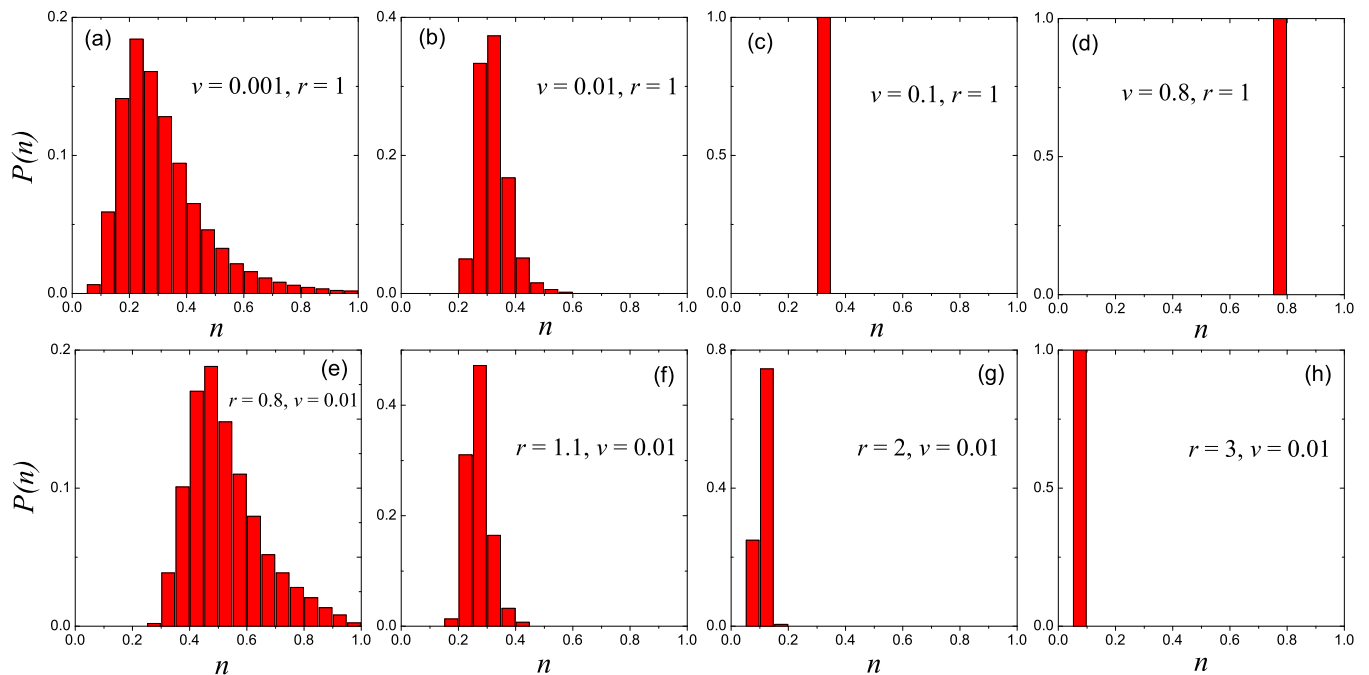


FIG. 5: (Color online) The load distribution  $P(n)$  vs  $n$  for different values of the moving speed  $v$  and the communication radius  $r$ . The packet-generation rate  $R = 100$ . From (a) to (d),  $v$  is 0.001, 0.01, 0.1, 0.8 respectively and  $r$  is fixed to be 1. From (e) to (h),  $r$  is 0.8, 1.1, 2, 3 respectively and  $v$  is fixed to be 0.01.

$\langle T \rangle$  increases as  $R$  increases. Due to the randomness of movement and packet generation, the number of packets in an agent's queue fluctuates as time evolves. At a time, if the number of packets in an agent's queue exceeds the agent's delivering ability, extra packets must wait for being delivered in the next time step. As  $R$  increases, the above phenomenon of transient congestion occurs more frequently, leading to a longer  $\langle T \rangle$ . For a fixed value of  $R$ , we find that  $\langle T \rangle$  keeps almost unchanged when the moving speed  $v$  increases from 0.001 to 0.1 [see Fig. 4(a)]. But as  $v$  continually increases,  $\langle T \rangle$  increases. As is shown in Fig. 4(a), for the same  $R$ , the average traveling time  $\langle T \rangle$  increases as  $v$  increases from 0.1 to 0.7. Figure 4(b) shows the average traveling time  $\langle T \rangle$  as function of  $R$  for different values of the communication radius  $r$ . One can see that, for the same value of  $R$ ,  $\langle T \rangle$  decreases as  $r$  increases.

Figure 5 shows the load distribution  $P(n)$  vs  $n$  for different values of  $v$  and  $r$ , where  $n$  represents the load and  $P(n)$  is the probability that an agent has the load  $n$ . We define an agent's load  $n_i$  as:

$$n_i = \frac{\sum n_i(t)}{\Delta T}, \quad (6)$$

where  $n_i(t)$  is the number of packets staying in  $i$ 's queue at time  $t$ ,  $\Delta T$  is period of time (we set  $\Delta T = 5 \times 10^4$ ) and the sum runs over a period of time  $\Delta T$ . An agent's load  $n_i$  reflects the average number of packets staying in  $i$ 's queue at a time.

Figures 5(a)-(d) show the load distribution  $P(n)$  for different values of the moving speed  $v$  when the packet-generation rate  $R = 100$  and the communication radius  $r = 1$ . One can see that,  $P(n)$  approximately displays the Poisson distribution when  $v$  is very small (i.e.,  $v = 0.001$  and  $v = 0.01$ ). As  $v$  increases (i.e.,  $v = 0.1$  and  $v = 0.8$ ), the load distribution becomes highly homogeneous and all agents have almost the same load. The highest load of an agent decreases as  $v$  increases from  $v = 0.001$  to  $v = 0.1$  [see Figs. 5(a)-(c)]. It is noted that for the same packet-generation rate, the average traveling time  $\langle T \rangle$  keeps almost unchanged for  $v = 0.001$  and  $v = 0.1$  [see Fig. 4(a)]. Thus, the change of the highest load for  $v = 0.001$  and  $v = 0.1$  is caused by the alteration of network structures. As the moving speed increases, each agent's neighbors change more frequently and the topology of network turns from quasistatic structure to dynamical structure. When  $v$  increases from 0.1 to 0.8, the average traveling time  $\langle T \rangle$  increases and the load of an agent enhances [see Figs. 5 (c) and (d)]. Since all agents have the same delivering ability  $C$ , the transportation capacity of the whole network is determined by the highest load of an agent. The increase of the highest load indicates that the decrease of the network's transportation capacity. Combining Fig. 4(a) with Figs. 5(a)-(d), we can understand why the highest transportation capacity of networks is reached at the moderate value of the moving speed.

Figures 5(e)-(h) show the load distribution  $P(n)$  for

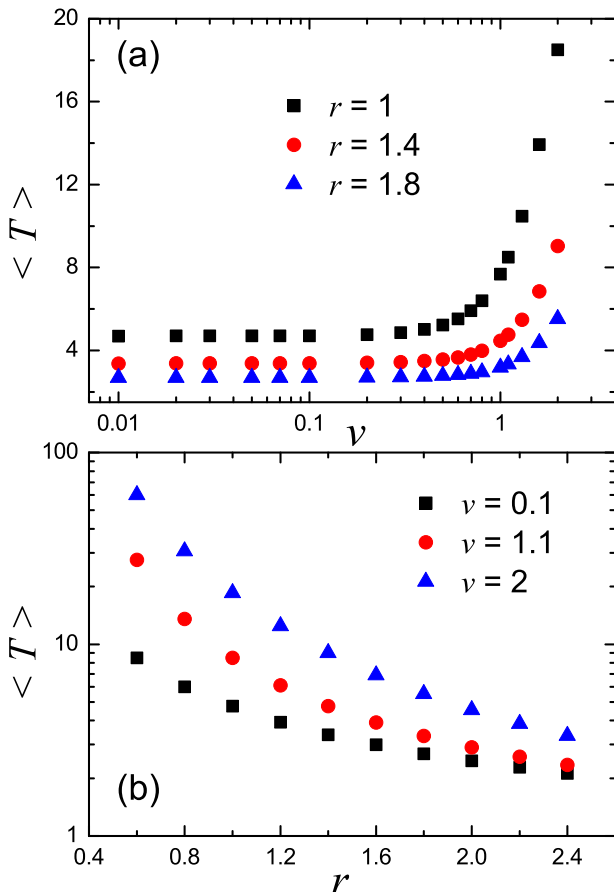


FIG. 6: (Color online) (a) The average traveling time  $\langle T \rangle$  as a function of the moving speed  $v$  for different values of the communication radius  $r$ . (b) The dependence of  $\langle T \rangle$  on  $r$  for different values of  $v$ .

different values of  $r$  when  $v$  is fixed to be 0.01. One can observe that,  $P(n)$  changes from the approximate Poisson distribution to highly homogeneous distribution as the communication radius  $r$  increases. Besides, the highest load of an agent decreases as  $r$  increases. According to Fig. 4(b), for the same packet-generation rate, the average traveling time  $\langle T \rangle$  decreases as  $r$  increases. The decrease of  $\langle T \rangle$  shortens the time steps that a packet stays in the system and relieves the traffic load, leading to the enhancement of the network's transportation capacity. Thus the phenomenon observed in Fig. 3(b) can be explained.

#### IV. EPIDEMIC SPREADING

In this section, we study how the greedy routing affects the traffic-driven epidemic spreading. We first consider the case where each agent's delivering ability is infinite,  $C \rightarrow \infty$ , so that traffic congestion will not occur in the network.

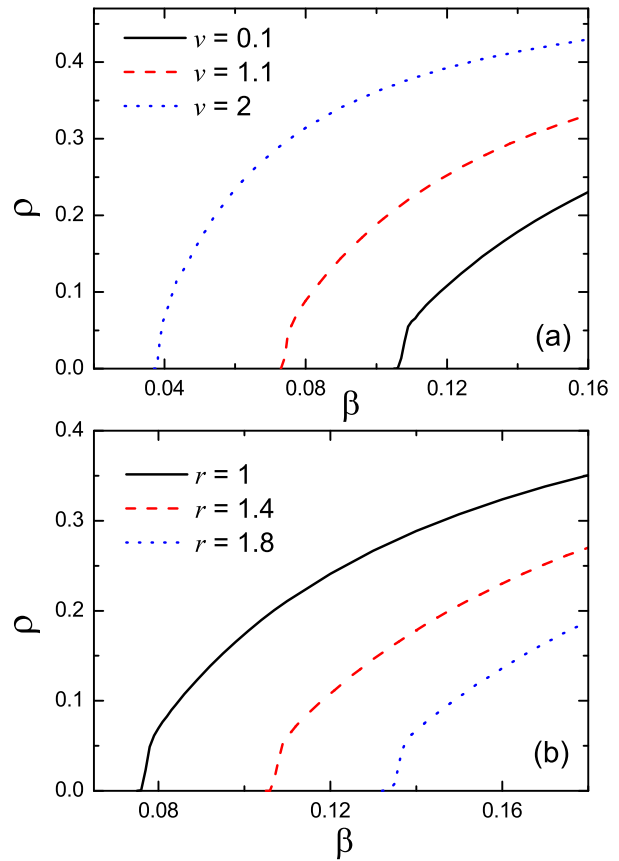


FIG. 7: (Color online) (a) Density of infected agents  $\rho$  as a function of the spreading rate  $\beta$  for different values of the moving speed  $v$ . The communication radius  $r = 1.4$ . (b) Density of infected agents  $\rho$  as a function of  $\beta$  for different values of  $r$ . The moving speed  $v = 0.1$ . The packet-generation rate is  $R = 4000$  and each agent's delivering ability is infinite. Each curve results from an average over 50 different realizations.

In the case of infinite delivering ability, the average traveling time  $\langle T \rangle$  is independent of packet-generation rate  $R$ . Figure 6 shows the dependence of  $\langle T \rangle$  on the moving speed  $v$  and the communication radius  $r$ . For a fixed value of  $r$ ,  $\langle T \rangle$  keeps almost unchanged for  $v < 0.3$  but increases as  $v$  continually increases [see Fig. 6(a)]. For a fixed value of  $v$ ,  $\langle T \rangle$  decreases as  $r$  increases [see Fig. 6(b)].

Figure 7 shows the density of infected agents  $\rho$  as a function of the spreading rate  $\beta$  for different values of the moving speed  $v$  and the communication radius  $r$ . We observe that, there exists an epidemic threshold  $\beta_c$ , beyond which the density of infected agents  $\rho$  is nonzero and increases as  $\beta$  is increased. For  $\beta < \beta_c$ , the epidemic dies out and  $\rho = 0$ . From Fig. 7, one can find that both  $v$  and  $r$  can affect the density of infected agents and the epidemic threshold. Large values of  $v$  and small values of  $r$  promote the epidemic spreading.

Figure 8(a) shows the epidemic threshold  $\beta_c$  as a function of the moving speed  $v$  for different values of the

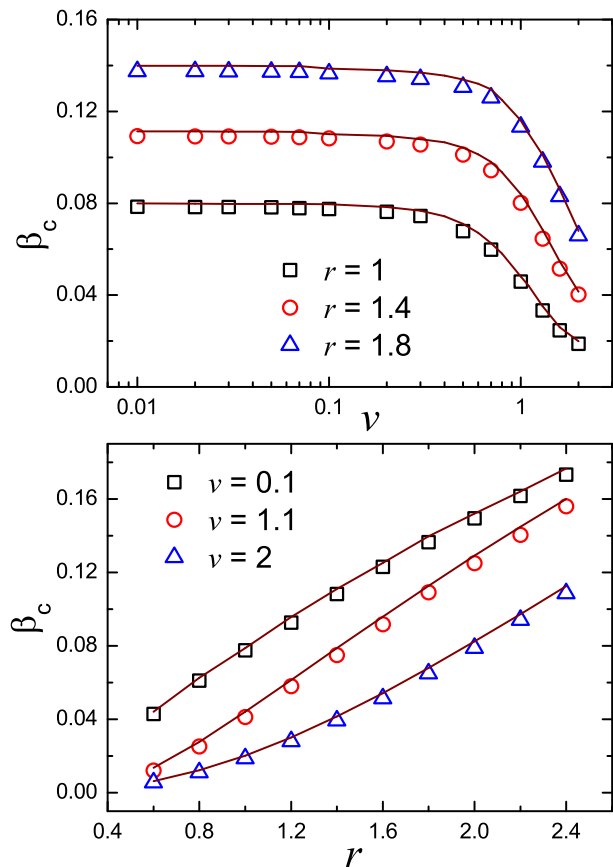


FIG. 8: (Color online) (a) Epidemic threshold  $\beta_c$  as a function of the moving speed  $v$  for different values of the communication radius  $r$ . (b) Epidemic threshold  $\beta_c$  vs  $r$  for different values of  $v$ . The packet-generation rate  $R = 4000$  and each agent's delivering ability is infinite. Each data point results from an average over 50 different realizations. The curves are theoretical predictions from Eq. (9).

communication radius  $r$ . One can see that, for a fixed value of  $r$ ,  $\beta_c$  keeps almost unchanged for  $v < 0.3$  but decreases as  $v$  continually increases. Figure 8(b) shows the dependence of  $\beta_c$  on  $r$  for different values of  $v$ . One can observe that  $\beta_c$  increases as  $r$  increases. In the following, we will provide a theoretical analysis to calculate the epidemic threshold  $\beta_c$ .

Since all agents have the same communication radius  $r$  and the load distribution  $P(n)$  follows the approximate Poisson distribution or highly homogeneous distribution, the mean-field theory can be applied. At each time step, the average number of packets that an agent delivers is  $R\langle T\rangle/N$ . Thus the rate equation for the epidemic dynamics can be written as

$$\frac{d\rho(t)}{dt} = -\rho(t) + \frac{R\langle T\rangle}{N}\beta\rho(t)[1 - \rho(t)]. \quad (7)$$

After imposing the stationarity condition  $d\rho(t)/dt = 0$ ,

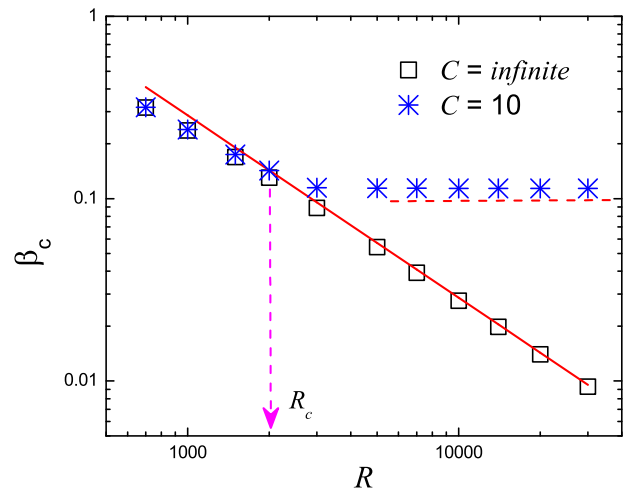


FIG. 9: (Color online) Epidemic threshold  $\beta_c$  as a function of the packet-generation rate  $R$  for  $C = 10$  and  $C \rightarrow \infty$ . The moving speed  $v = 0.5$  and the communication radius  $r = 1$ . For  $C = 10$ , the critical packet-generating rate  $R_c$  is about 2000. Each data point results from an average over 50 different realizations. The solid and dash line is the theoretical prediction from Eq. (9) and Eq. (11), respectively.

we obtain

$$\rho[-1 + \frac{R\langle T\rangle}{N}\beta(1 - \rho)] = 0. \quad (8)$$

From Eq.(8), we get the epidemic threshold

$$\beta_c = \frac{N}{R\langle T\rangle}. \quad (9)$$

The comparison between numerical and theoretical values of  $\beta_c$  is shown in Fig. 8 (we use the numerical values of  $\langle T\rangle$  in Eq. (9) because of the difficulty in calculating  $\langle T\rangle$  theoretically). From Fig. 8, we find that the theoretical prediction of  $\beta_c$  is in good agreement with that of simulation result.

Next, we consider the finite delivery ability. In this case, traffic congestion occurs when the packet-generation rate  $R$  is above a critical value  $R_c$ . Figure 9 shows the epidemic threshold  $\beta_c$  as a function of  $R$  for  $C = 10$  and  $C \rightarrow \infty$ . One can see that,  $\beta_c$  scales inversely with the  $R$  for  $C \rightarrow \infty$ , as predicted by Eq. (9). For  $C = 10$ ,  $\beta_c$  decreases to a steady value as  $R$  increases. When  $R \leq R_c$ ,  $\beta_c$  is almost the same for finite and infinite delivery ability. However, for  $R > R_c$ , we observe that the value of  $\beta_c$  is larger for  $C = 10$  than that of  $C \rightarrow \infty$ , indicating that traffic congestion can suppress the spreading of disease. Similar phenomena were also been found in Refs. [5, 14].

In the case of finite delivery ability, the lower limit of the epidemic threshold can be estimated as follows.

For sufficiently large values of  $R$ , all agents will become congested and each agent can deliver only  $C$  packets at each time step. Thus Eq. (7) must be revised as

$$\frac{d\rho(t)}{dt} = -\rho(t) + C\beta\rho(t)[1 - \rho(t)]. \quad (10)$$

Imposing the stationarity condition  $d\rho(t)/dt = 0$  and we obtain the epidemic threshold

$$\beta_c = \frac{1}{C}. \quad (11)$$

## V. CONCLUSION

In conclusion, we studied how greedy routing affects traffic dynamics and traffic-driven epidemic spreading on networks of mobile agents. Our main findings are the following. Firstly, for finite delivering ability, the transportation capacity of networks peaks at the moderate moving speed and increases as the communication radius increases. Secondly, the average traveling time of a packet increases as the moving speed increases but decreases as the communication radius increases. Thirdly,

for infinite delivering ability, the epidemic threshold decreases as the moving speed increases and increases as the communication radius increases. Fourthly, traffic congestion can suppress epidemic spreading. Since the study of networks of mobile agents has received increasing attention in recent years, our results are valuable for understanding the structure and dynamics of mobile networks.

## Acknowledgments

HXY and BHW were funded by by the National Important Research Project (Grant No. 91024026), the National Natural Science Foundation of China (No. 10975126), and the Specialized Research Fund for the Doctoral Program of Higher Education of China (No. 20093402110032). WXW and YCL were supported by AFOSR under Grant No. FA9550-10-1-0083 and by NSF under Grants No. BECS-1023101 and No. CDI-1026710.

- 
- [1] R. Pastor-Satorras and A. Vespignani, *Evolution and Structure of the Internet: A Statistical Physics Approach* (Cambridge University Press, Cambridge, 2004).
- [2] J.-P. Onnela, J. Saramäki, J. Hyvönen, G. Szabó, D. Lazer, K. Kaski, J. Kertész, and A.-L. Barabási, *Proc. Natl. Acad. Sci. USA* **104**, 7332 (2007).
- [3] R. Guimerà, A. Díaz-Guilera, F. Vega-Redondo, A. Cabrales, and A. Arenas, *Phys. Rev. Lett.* **89**, 248701 (2002); B. J. Kim, C. N. Yoon, S. K. Han, and H. Jeong, *Phys. Rev. E* **65**, 027103 (2002); B. Tadić, S. Thurner, and G. J. Rodgers, *Phys. Rev. E* **69**, 036102 (2004); V. Cholvi, V. Laderas, L. López, and A. Fernández, *Phys. Rev. E* **71**, 035103(R) (2005); B. K. Singh and N. Gupte, *Phys. Rev. E* **71**, 055103(R) (2005); M.-B. Hu, W.-X. Wang, R. Jiang, Q.-S. Wu, and Y.-H. Wu, *Phys. Rev. E* **75**, 036102 (2007); X. Ling, M.-B. Hu, R. Jiang, R. Wang, X.-B. Cao, and Q.-S. Wu, *Phys. Rev. E* **80**, 066110 (2009); M. Tang, Z. Liu, X. Liang, and P. M. Hui, *Phys. Rev. E* **80**, 026114 (2009).
- [4] R. Pastor-Satorras and A. Vespignani, *Phys. Rev. Lett.* **86**, 3200 (2001); R. Pastor-Satorras and A. Vespignani, *Phys. Rev. E* **65**, 035108(R) (2002); M. E. J. Newman, *Phys. Rev. E* **66**, 016128 (2002); R. Cohen, S. Havlin, and D. ben-Avraham, *Phys. Rev. Lett.* **91**, 247901 (2003); V. Colizza, R. Pastor-Satorras, and A. Vespignani, *Nat. Phys.* **3**, 276 (2007); J. G. Gardeñes, V. Latora, Y. Moreno, and E. Profumo, *Proc. Natl. Acad. Sci. USA* **105**, 1399 (2008). M. Tang, L. Liu, and Z. Liu, *Phys. Rev. E* **79**, 016108 (2009); C. Castellano and R. Pastor-Satorras, *Phys. Rev. Lett.* **105**, 218701 (2010); S. Gómez, J. Gómez-Gardeñes, Y. Moreno, and A. Arenas, *Phys. Rev. E* **84**, 036105 (2011).
- [5] S. Meloni, A. Arena, and Y. Moreno, *Proc. Natl. Acad. Sci. USA* **106**, 16897 (2009).
- [6] N. T. J. Bailey, *The Mathematical Theory of Infectious Diseases* (Griffin, London, 1975).
- [7] M. E. J. Newman, *Phys. Rev. E* **64**, 016132 (2001).
- [8] L. Zhao, Y.-C. Lai, K. Park, N. Ye, *Phys. Rev. E* **71**, 026125 (2005).
- [9] P. Echenique, J. Gómez-Gardeñes, and Y. Moreno, *Phys. Rev. E* **70**, 056105 (2004); *Europhys. Lett.* **71**, 325 (2005).
- [10] W.-X. Wang, B.-H. Wang, C.-Y. Yin, Y.-B. Xie, and T. Zhou, *Phys. Rev. E* **73**, 026111 (2006).
- [11] G. Yan, T. Zhou, B. Hu, Z.-Q. Fu, and B.-H. Wang, *Phys. Rev. E* **73**, 046108 (2006).
- [12] M. Boguñá, D. Krioukov, and K. C. Claffy, *Nat. Phys.* **5**, 74 (2009).
- [13] S. Meloni, N. Perra, A. Arenas, S. Gómez, Y. Moreno, and A. Vespignani, *Scientific Reports* **1**, 62 (2011).
- [14] H.-X. Yang, W.-X. Wang, Y.-C. Lai, Y.-B. Xie, and B.-H. Wang, *Phys. Rev. E* **84**, 045101(R) (2011).
- [15] H.-X. Yang, W.-X. Wang, Y.-B. Xie, Y.-C. Lai, and B.-H. Wang, *Phys. Rev. E* **83**, 016102 (2011).
- [16] A. Arenas, A. Díaz-Guilera, and R. Guimerà, *Phys. Rev. Lett.* **86**, 3196 (2001).